

# Effect of Turbulence Intensity on Turning Diffuser Performance at Various Angle of Turns


 Open  
Access

Lim Gim Huang<sup>1</sup>, Normayati Nordin<sup>1,\*</sup>, Lim Chia Chun<sup>1</sup>, Nur Shafiqah Abdul Rahim<sup>1</sup>, Shamsuri Mohamed Rasidi<sup>1</sup>, Muhammad Zahid Firdaus Shariff<sup>1</sup>

<sup>1</sup> Centre for Energy and Industrial Environment Studies, Faculty of Mechanical and Manufacturing Engineering, Universiti Tun Hussein Onn Malaysia, 86400 Parit Raja, Johor, Malaysia

## ARTICLE INFO

### Article history:

Received 22 November 2019  
 Received in revised form 18 January 2020  
 Accepted 23 January 2020  
 Available online 31 January 2020

### Keywords:

3-D turning diffuser; turbulence intensity; pressure recovery coefficient; flow uniformity; Computational Fluid Dynamics (CFD)

## ABSTRACT

The performances of turning diffuser are highly affected due to the nature of its geometries by the existence of flow separation and dispersion of core and secondary flows. Turning diffusers with potential turbulence intensity may lead to optimum performance. However, there has been yet insufficient literature on 3-D turning diffuser fluid flow performance analysis by varying inlet turbulence intensity. Hence, this study aims to investigate the effect of turbulence intensity on 30° and 90° 3-D turning diffuser performances. The performances of turning diffusers were scientifically evaluated in term of pressure recovery coefficient,  $C_p$  and flow uniformity index,  $\sigma_{out}$  while turbulence intensity was varied from 1.5% to 7.5%. This work involved both numerical and experimental methods. ANSYS Computational Fluid Dynamics (CFD) was used for the simulation and Particle Image Velocimetry (PIV) for the experiment. The inlet free-stream turbulence intensity was varied which imposed on the flow by suppressing the separation of the inner wall boundary layer and mixing to provide optimum uniformity of the flow. The pressure recovery increased 8.02% and 9.74% while the flow uniformity improved about 2.95% and 1.60% in 30° case and 90° case respectively. In conclusion, the 7.5% of turbulence intensity is promising to introduce in the ducting flow application so as to improve the pressure recovery and the flow uniformity of both 30° and 90° turning diffuser cases.

Copyright © 2020 PENERBIT AKADEMIA BARU - All rights reserved

## 1. Introduction

Diffuser is a common fluid flow device with relatively large outlet cross-section to the inlet often applied to decrease the velocity and increase the static pressure. It acts as an energy converter to transform kinetic energy of fluid passing through it to potential energy of pressure. A diffuser with no turn is known as a straight diffuser, whereas with certain angle of turn known as a turning diffuser. Turning diffuser is often introduced in ducting or piping systems due to design compatibility and

\* Corresponding author.

E-mail address: [mayati@uthm.edu.my](mailto:mayati@uthm.edu.my) (Normayati Nordin)

space restriction [1]. It is applied widely in heating, ventilation and air conditioning (HVAC) system as an adapter to interconnect two different cross sectional area of conduits [2].

These diffuser performances would be affected due to improper setting of geometrical and operating parameters that had caused flow separation to occur to distort the optimum flow performance [3 -7]. There was a promising improvement in terms of 55° turning diffuser performance in relative to straight diffuser when appropriate turbulent intensity, 3.4% was applied by Sullerey *et al.*, [6]. The performance guideline established by Fox & Kline [4] for turning diffuser however is restricted to 2-D case. In addition, no works have been done so far to comprehensively investigate the effect of turbulent intensity on the performance of 3-D turning diffuser [7-10]. In the present work, the effect of turbulence intensity on 30° and 90° 3-D turning diffuser performance is numerically investigated.

## 2. Methodology

### 2.1 Performance Index

The performance of diffuser can be generally evaluated in terms of pressure recovery coefficient ( $C_p$ ) and flow uniformity index ( $\sigma_{out}$ ) as presented in Eq. (1) and Eq. (2), respectively.

$$C_p = \frac{2(P_{outlet} - P_{inlet})}{\rho V_{inlet}^2} \quad (1)$$

where  $P_{outlet}$ ,  $P_{inlet}$ ,  $\rho$  and  $V_{inlet}$  respectively are average static pressure at diffuser outlet (Pa), average static pressure at diffuser inlet (Pa), density of air ( $\text{kg}/\text{m}^3$ ) and mean velocity of inlet air (m/s).

$$\sigma_{out} = \sqrt{\frac{1}{N-1} \sum_{i=1}^N (V_i - V_{out})^2} \quad (2)$$

where  $N$ ,  $V_{out}$ ,  $V_i$  are number of measurement points, local outlet air velocity (m/s) and mean outlet air velocity (m/s) respectively.

### 2.2 Modelling

Turning diffusers with angle of turn,  $\theta = 30^\circ$  and  $90^\circ$ , identical geometrical parameters of  $AR = 2.16$ ,  $W_2/W_1=1.44$ ,  $X_2/X_1=1.50$ ,  $L_{in}/W_1=3.99$  were modeled using SolidWorks 2016 as shown in Figure 1.

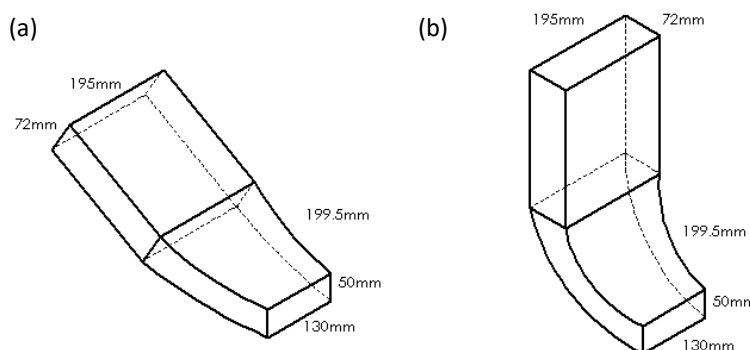


**Fig. 1.** Schematic diagram of 3D turning diffuser with turning angle of (a) 30° and (b) 90°

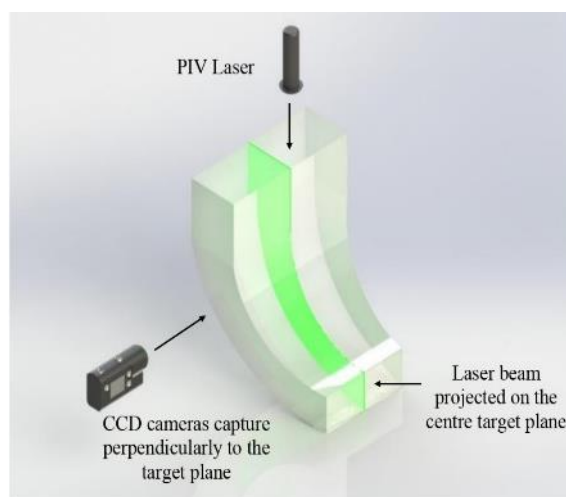
### 2.3 Experimental Works

The experimental rig as shown in Figure 2 was developed to consist of turning diffuser, settling chamber, screening mesh nets, bellow and 3-phase inverter control centrifugal blower. Approximated 2 meters of hydrodynamic entrance length was introduced before the actual inlet to ensure the fully developed turbulence flow. Meanwhile, pitot static system was used to determine the local velocity at 7 equivalent distance points across perpendicularly to the fluid flow while the velocity profile was presented a flattening flow profile. These local velocities were compared with the theoretical velocities calculated with Seventh Power Law while the deviation percentages was recorded less than 5%.



**Fig. 2.** The development of experimental rig

The 2-D PIV measurement was conducted to obtain the velocity vector and flow regime for both turning diffuser at center plane while calibrated camera mounted was directed perpendicularly to laser projection plane as shown in Figure 3(a) [11]. For the measurement of pressure recovery, four holes with 2 mm diameter were drilled at the actual inlet and actual outlet of the turning diffuser respectively. Figure 3(b) presents the holes were tapping with tubes connecting with three T-shaped adapter before connected to the air flow meter in order to measure the average static pressures of  $P_{inlet}$  and  $P_{outlet}$  precisely and the connecting method of air flow meter with T-shaped adapters and tubes tapping. The pressure recovery was calculated with Eq. (1) and tabulated in Table 1. The  $C_p$  results of 30° and 90° turning diffuser were used for the validation purpose of simulation model and results.



(a)

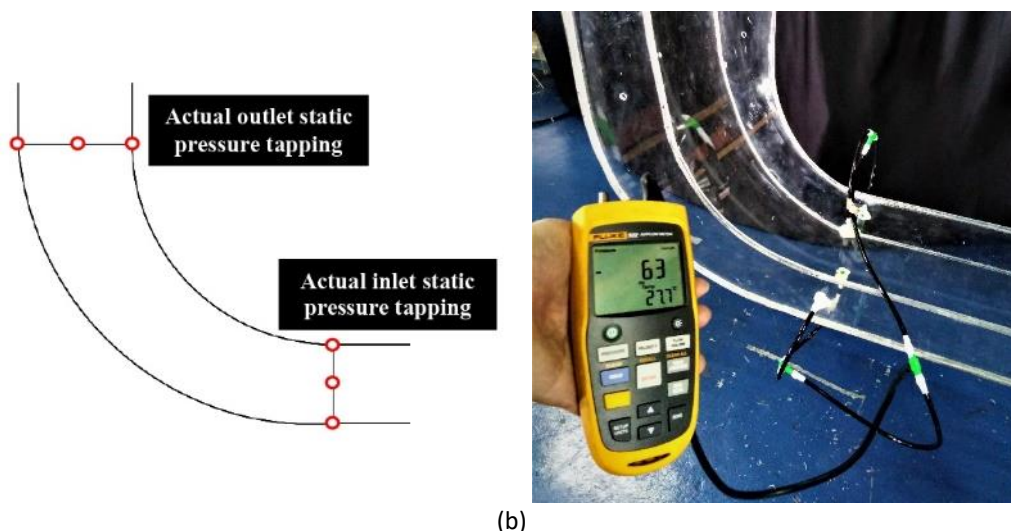


**Fig. 3.** (a) 2-D Particle Image Velocimetry and (b) measurement of average inlet and outlet static pressure setup

## 2.4 Meshing

ANSYS CFD 19.2 was used to perform the numerical works on the performances of the turning diffusers. A hybrid mesh of tetrahedron and hexahedron with skewness quality less than 0.3 was applied by enabling inflation method. As the low  $Re < 10^6$  was considered at this study, thus enhanced wall treatment applied while the wall-adjacent cell centroid was placed within the viscous sublayer,  $y^+ \approx 1.0$ . With the  $Re$  of  $6.4 \times 10^4$  and inlet velocity of 14.25 m/s, the corresponding first grid point off the wall was calculated as  $2.278 \times 10^{-5} m$  with formula of  $y^+ = yu_\tau/v$ . The grid independency study was conducted by refining further the mesh elements until the  $C_p$  results show insignificant changes. Table 1 illustrates Mesh 4 provides the least deviation of  $C_p$  relative to the finest Mesh 5 in every case thus was chosen as an optimum mesh to be adopted in the intensive simulation.

**Table 1**  
Mesh independency study for 30° and 90° of 3D turning diffuser

Angle of Diffuser, $\phi$	Mesh	Nodes	Pressure recovery, $C_p$	Deviation (%)
30°	1	355218	0.3223	26.68
	2	400101	0.3561	18.99
	3	450847	0.3822	13.05
	4	508864	0.4238	3.59
	5	582750	0.4395	-
90°	1	350986	0.2488	22.56
	2	399694	0.2548	20.69
	3	453831	0.3031	5.69
	4	502766	0.3180	1.03
	5	574875	0.3213	-

## 2.5 Boundary Conditions

The inlet velocity was initially set at 14.25 m/s and  $Re_{in}$  was calculated as  $6.382 \times 10^4$ . The outlet pressure was assumed as atmospheric pressure at 1 atm. The inlet turbulent intensity,  $I_{in}$  was initially set as 4.0 %. The smooth solid wall was taken into consideration and temperature of working fluid

was set at 30°C. The working fluid was air at 30°C with  $\rho = 1.164 \text{ kg/m}^3$  and  $\mu = 1.872 \times 10^{-5} \text{ kg/m.s}$ . Table 2 listed the boundary operating conditions.

**Table 2**

Boundary operating conditions

Inlet	Type of boundary	Velocity-inlet
	Velocity magnitude, $V_{in}$ (m/s)	14.25 ( $Re_{in} = 6.382 \times 10^4$ )
	Turbulent intensity, $I_{in}$ (%)	4.0
	Hydraulic diameter, $D_h$ (mm)	72.22
Outlet	Type of boundary	Pressure-outlet
	Pressure (Pa)	0 gauge pressure
Wall	Type of boundary	Smooth wall
	Shear condition	No-slip

## 2.6 Governing Equations

The standard k- $\epsilon$  model (std k- $\epsilon$ ) with double precision pressure-based solver was used to solve the RANS equations [12-15]. Pressure-linked equation with semi-implicit method SIMPLE was applied. The SIMPLE algorithm has been derived from the combination of continuity equation and the momentum equation in order to derive pressure equation. The solution for the gradient is occupied by Green-Gauss-Cell based while QUICK-type scheme was exploited for the momentum equations, turbulent dissipation rate equation and turbulent kinetic energy equation. A convergence value of  $10^{-5}$  was suggested as the residual error for all the governing equations in this study.

## 2.7 Intensive Simulation

The intensive simulations were performed to investigate the effects of varying turbulence intensity, 1.5% to 7.5% on the performance of 30° and 90° 3-D turning diffusers. The performances of turning diffuser were considered and discussed on the pressure recovery coefficient, flow uniformity index and flow separation.

## 3. Results and Discussion

### 3.1 Experimental Results

#### 3.1.1 Verification of full developed flow

Approximated 2 meters of hydrodynamic entrance length was introduced at the turning diffuser before the actual inlet to ensure the fully developed turbulence flow. Meanwhile, pitot static system was used to determine the local velocity at 7 equivalent distance points across perpendicularly to the fluid flow where the localized velocity was recorded. Verification of fully developed fluid flow has been determined where flattening velocity profile is shown in Figure 4 with data obtained. The Seventh Power Law was used to calculate the theoretical velocities,  $V_{in\ theo}$  along the fluid flow. These had shown strong and supportive agreement with experimental results which the deviation percentages are less than 8%.

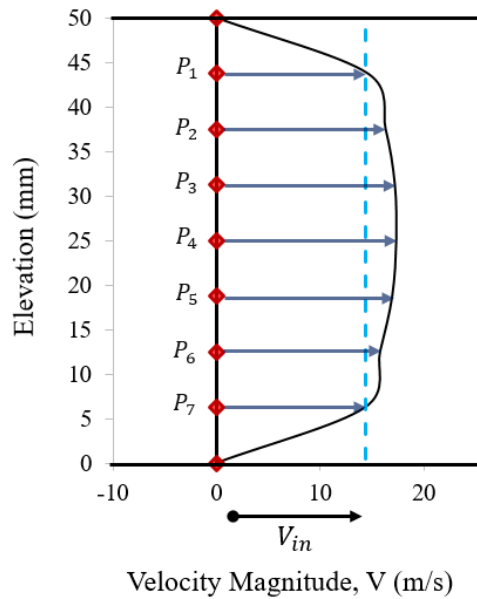


**Fig. 4.** Verified fully developed turbulent flow profile

### 3.1.2 2-D Particle image velocimetry

2-D PIV was applied to obtain the flow regime structure and velocity vector along longitudinal section of 30° and 90° turning diffusers as shown in Figure 5. These flow vectors were used for the comparison of CFD validation purposes.

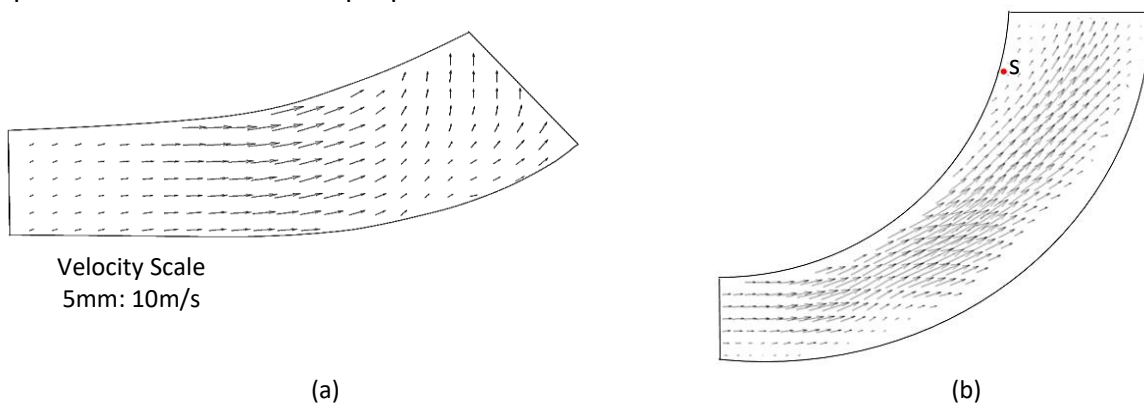


**Fig. 5.** Velocity vector from PIV (a) 30° and (b) 90° turning diffusers

### 3.1.3 Pressure recovery coefficient

The inlet and outlet static pressures and the inlet dynamic pressure were initially measured in order to solve the  $C_p$ . Table 3 tabulates the experimental  $C_p$  results for both 30° and 90° turning diffuser.

**Table 3**  
Experimental  $C_p$  results of turning diffusers

Angle of Diffuser, $\phi$	Static Pressure, (kPa)		Dynamics pressure, $P_{dyn}$ (kPa)	Pressure Recovery, $C_p$
	Inlet, $P_{inlet}$	Outlet, $P_{outlet}$		
30°	-68.0	-11.0	123.91	0.460
90°	-62.0	-19.0	123.95	0.347

### 3.2 Validation of CFD Simulation with Experiment

CFD validation was conducted by comparing the numerical result of pressure recovery,  $C_p$  with experimental result. Table 4 shows that the CFD simulation results strongly agree with the experimental result as the deviation of both result is less than 6%. Figure 6 illustrates the comparison between the flow structure of 30° and 90° turning diffuser of experiment and CFD simulation using ske model. These comparisons conclude that the simulation results show reliable supportive evidence with both identical flow structures. With this optimum results, the turbulence model of standard k- $\epsilon$  (ske) is selected for the intensive simulation by varying the turbulence intensity.

**Table 4**  
 Deviation of experimental and numerical pressure recovery,  $C_p$  results

Solver model	Angle of Diffuser, $\phi$	Pressure recovery, $C_p$		Deviation (%)
		Experimental	Numerical	
Standard k- $\epsilon$	30°	0.4599	0.4335	5.74
	90°	0.3470	0.3282	5.41

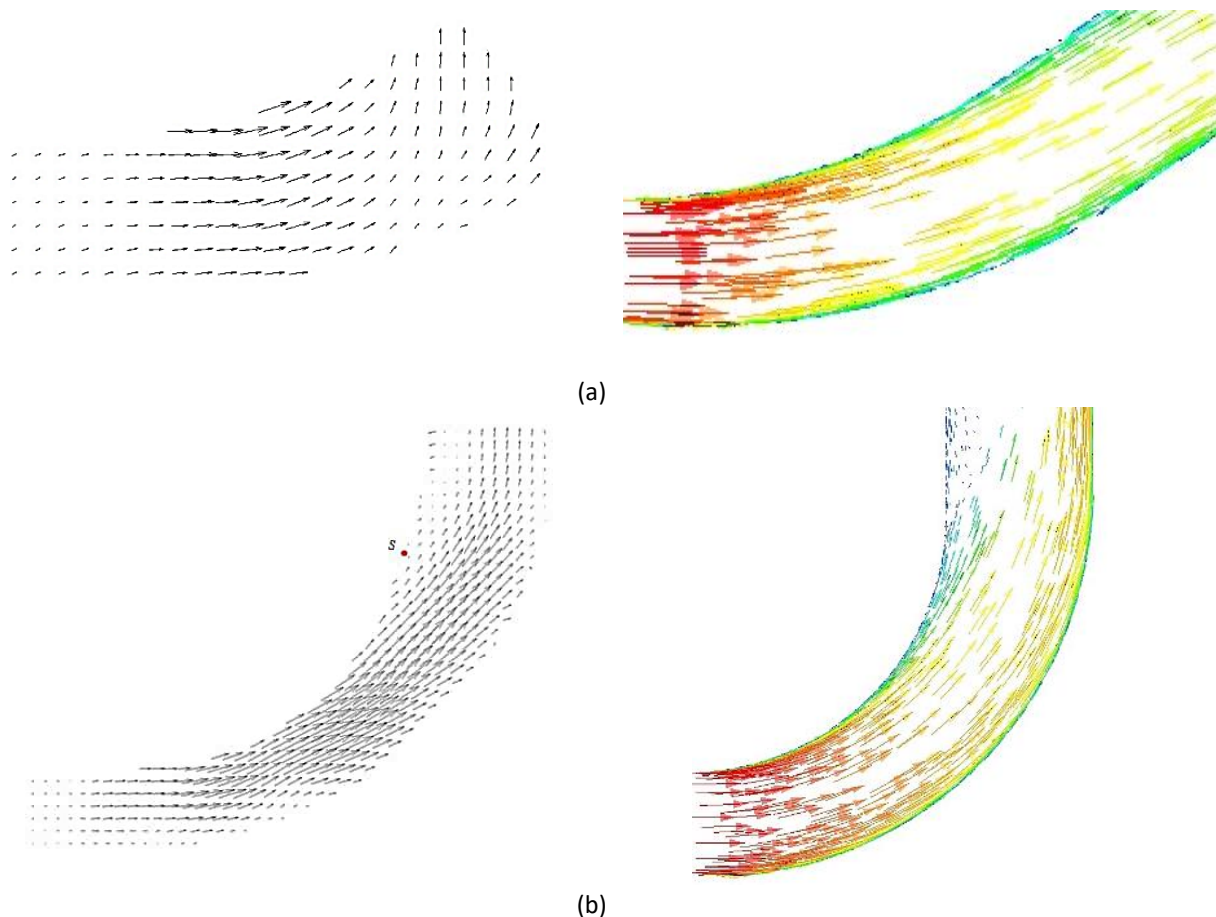


**Fig. 6.** Flow regime structure (a) 30° and (b) 90° turning diffuser in experiment (left side) and CFD simulation (right side)

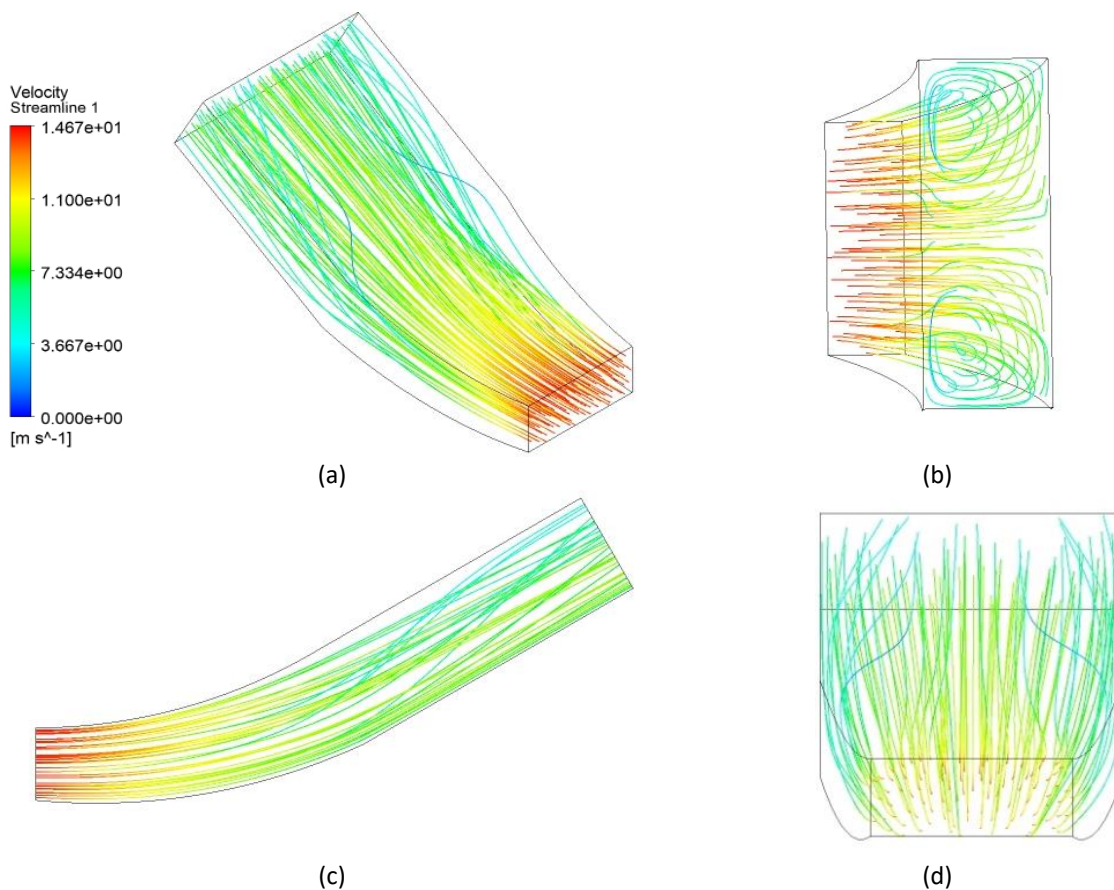
### 3.3 Effect of Turbulence Intensity on 30° Turning Diffuser

Table 5 summarizes the flow uniformity, pressure recovery and onset flow separation results of 30° turning diffuser by varying turbulence intensity. With the increment of turbulence intensity from

1.5% to 7.5%, the performance of pressure recovery and flow uniformity shows an enhancement of 8.02% and 2.95% respectively. The same findings have been shared by Hoffmann & Gonzalez in their research [5]. The swirling condition is meant to be observed at top and front view of the diffuser shown in Figure 7 which is the reason of affecting the flow performance with increasing the flow uniformity index. Increasing the intensity to maximum of 7.5% helps flow to resolve thus provides promising improvement of uniformity thus recovery as indicated in Figure 8.

**Table 5**  
 Effect of turbulence intensity on the 30° turning diffuser performance

Angle of Diffuser, $\phi$	Turbulence Intensity, $I$	Pressure recovery, $C_p$	Flow uniformity, $\sigma_{out}$	Separation point, S
30°	1.50	0.4098	2.9306	-
	3.00	0.4180	2.9103	-
	4.50	0.4269	2.8889	-
	6.00	0.4365	2.8667	-
	7.50	0.4456	2.8468	-



**Fig. 7.** Flow velocity streamline structure of 30° turning diffuser in varying turbulence intensity at (a) isometric view, (b) top view, (c) side view, (d) front view

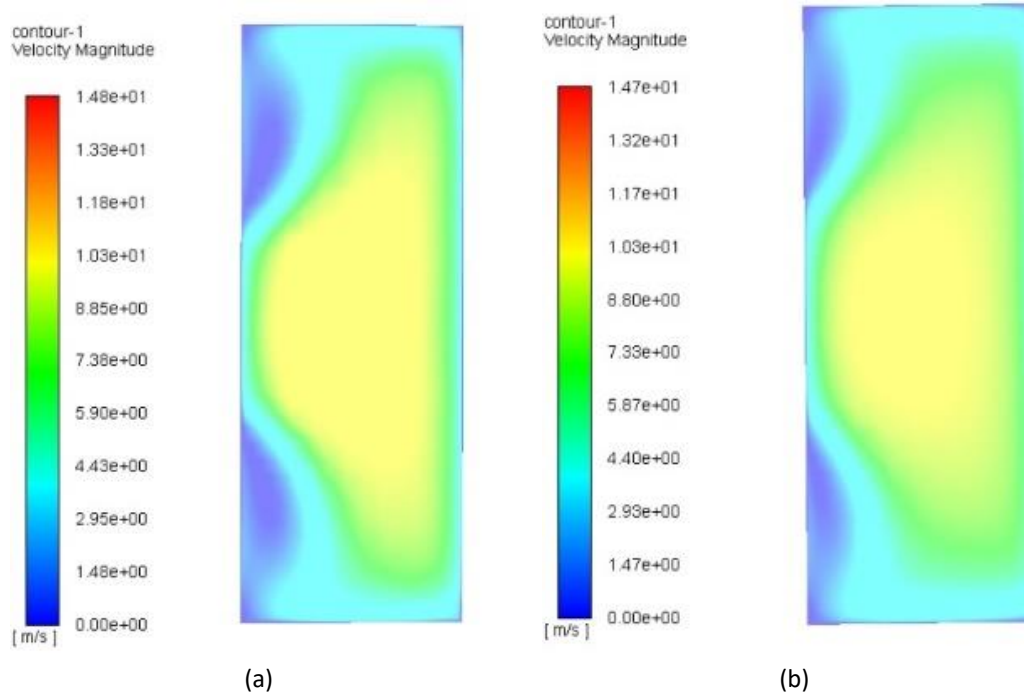


**Fig. 8.** Actual outlet velocity distribution in 30° turning diffuser with turbulence intensity of (a) 1.50% and (b) 7.50%

### 3.4 Effect of Turbulence Intensity on 90° Turning Diffuser

The pressure recovery and flow uniformity exhibit an increment of 9.74 % and 1.60 % respectively as summarized in Table 6 for 90° case via increasing the turbulent intensity in which Sullerey *et al.*, [6] also shared the same trend of results. In brief, the flow uniformity is strongly depending on the presence of core and secondary flow vortices throughout the cross-section of the outlet. The swirling and stall condition are meant to be observed at top and front view of Figure 9 which affect the flow performance. Velocity distribution at the actual outlet by varying the turbulence intensity are illustrated an improvement trend where the dispersion of core and secondary flow are diminished while the flow uniformity improves about 1.60 % indicated in Figure 10.

**Table 6**  
 Effect of turbulence intensity on the 90° turning diffuser performance

Angle of Diffuser, $\phi$	Turbulence Intensity, $I$	Pressure recovery, $C_p$	Flow uniformity, $\sigma_{out}$	Separation point, S
90°	1.50%	0.3074	3.5771	$0.93 L_{in}/W_1$
	3.00%	0.3130	3.5752	$0.93 L_{in}/W_1$
	4.50%	0.3208	3.5653	$0.93 L_{in}/W_1$
	6.00%	0.3303	3.5470	$0.93 L_{in}/W_1$
	7.50%	0.3405	3.5206	$0.93 L_{in}/W_1$

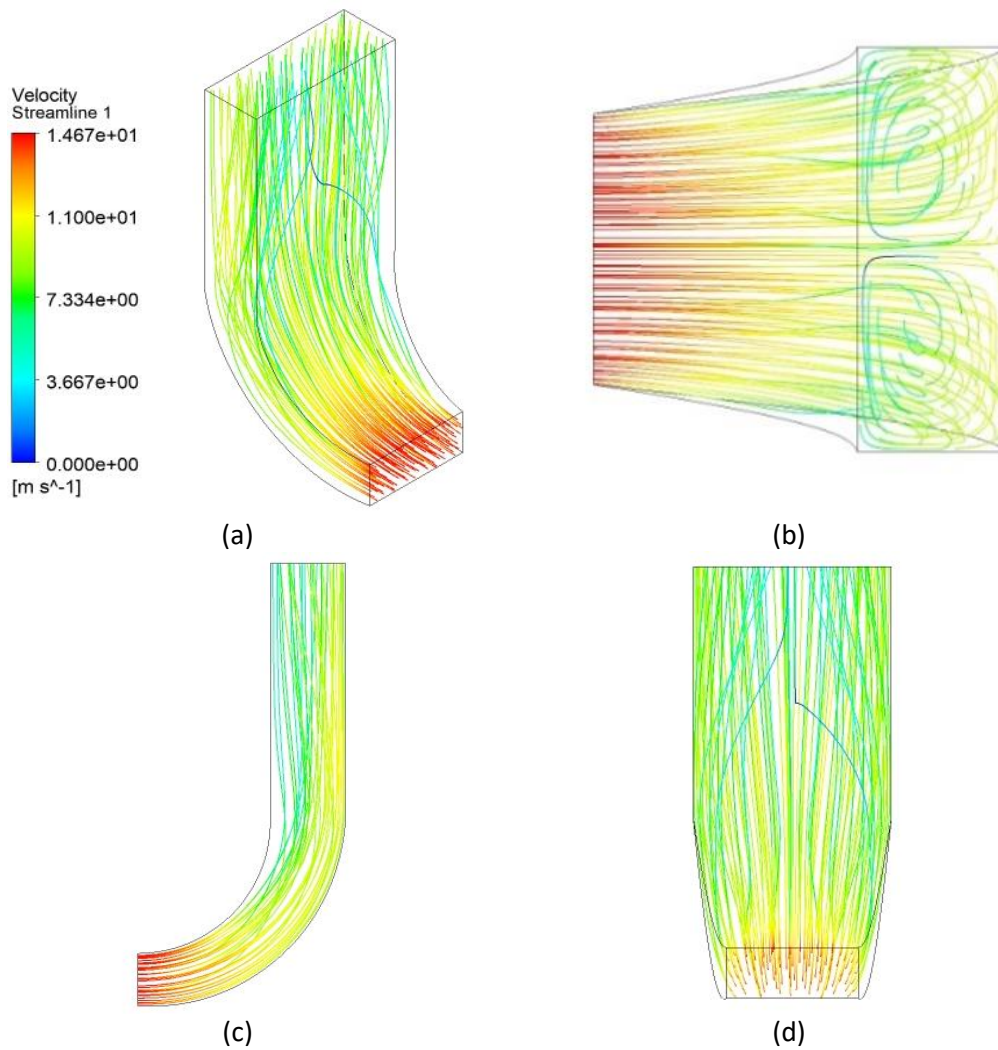


**Fig. 9.** Flow velocity streamline structure of 90° turning diffuser in varying turbulence intensity at (a) isometric view, (b) top view, (c) side view, (d) front view

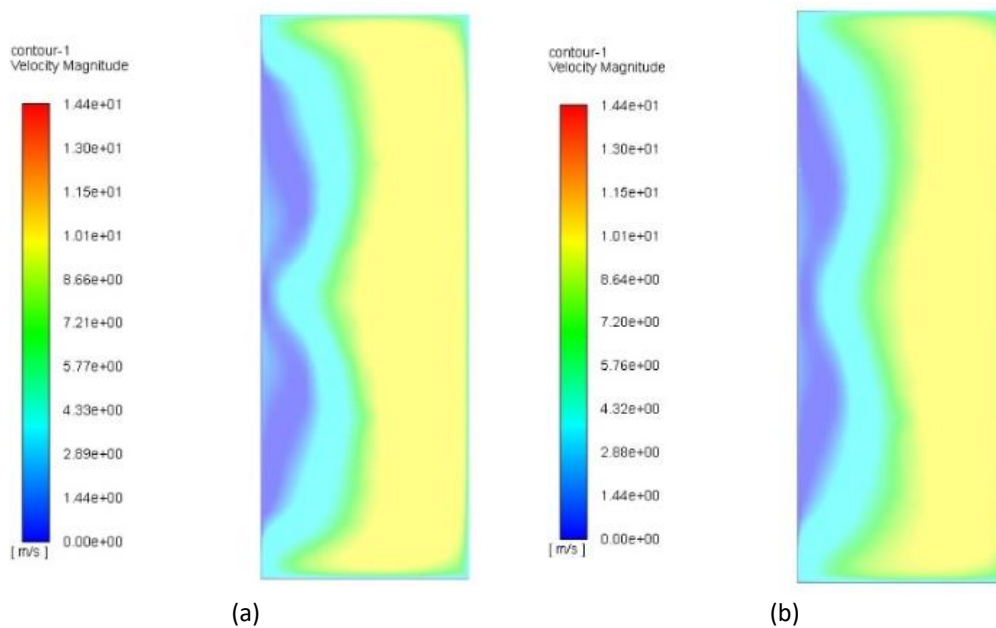


**Fig. 10.** Actual outlet velocity distribution in 90° turning diffuser with turbulence intensity of (a) 1.50% and (b) 7.50%

### 3.5 Results Comparison Between 30° and 90° Turning Diffuser

The improvement trend on both turning diffuser is observed in Figure 11 while an increasing gradient of 0.567 and 0.552 shown by  $C_p$  of 30° and 90° turning diffuser respectively. This shows that  $C_p$  in 30° turning diffuser is slightly higher than 90° in virtue of the geometry of turning diffuser and the viscous effect where the unfavorable adverse pressure gradient increases at the higher turning angle of the diffuser. The  $\sigma_{out}$  is strongly influenced by both core and secondary flow characteristics. Figure 12 illustrates that  $\sigma_{out}$  indexes decreases when increment of turbulence intensity. A decreasing gradient of 1.289 and 0.869 calculated from  $\sigma_{out}$  of 30° and 90° turning diffuser respectively. With this, we had observed that performance of 30° turning diffuser fluid flow is relatively higher than 90° due to the excessive losses on the viscous effect and swirling and reversible flow presented.

Moreover, the flow separation is only observed at  $0.93L_{in}/W_1$  of 90° turning diffuser case study whereas there is no flow separation in 30° turning diffuser case study as shown in Figure 13 [16-18]. These may due to the fluid at the central axis is subjected to the outer wall of the ducting when flowing through a bend and develops a radial pressure gradient due to centrifugal force imbalance. In 90° turning diffuser case study, the increment of  $I$  is not influenced or delayed the flow separation location along the ducting.

Furthermore, the outlet velocity profile at the center plane of 30° and 90° turning diffuser with 1.5% and 7.5% of  $I$  was illustrated in Figure 14. The 30° and 90° case study velocity profile with 1.5% of  $I$  illustrated local outlet velocity is slightly higher compared with 7.5% of  $I$  but the application of higher turbulence intensity showed more flattening velocity flow profile. This graph had proven that the higher turbulence intensity was able to improve the velocity distribution at the outlet of the diffuser.

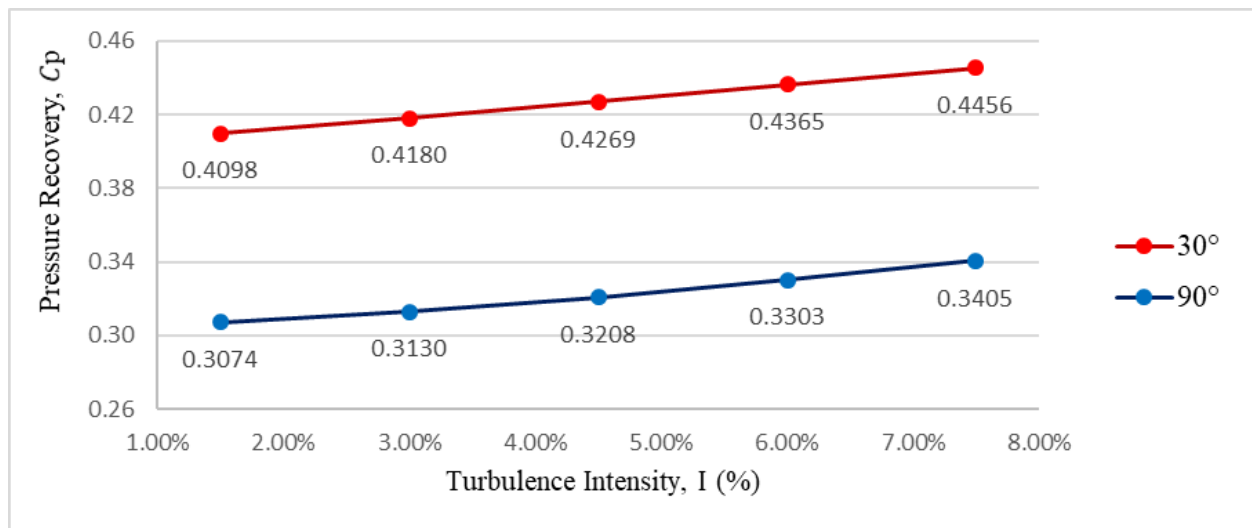


**Fig. 11.** Comparison of  $C_p$  versus  $I$  at 30° and 90° turning diffusers

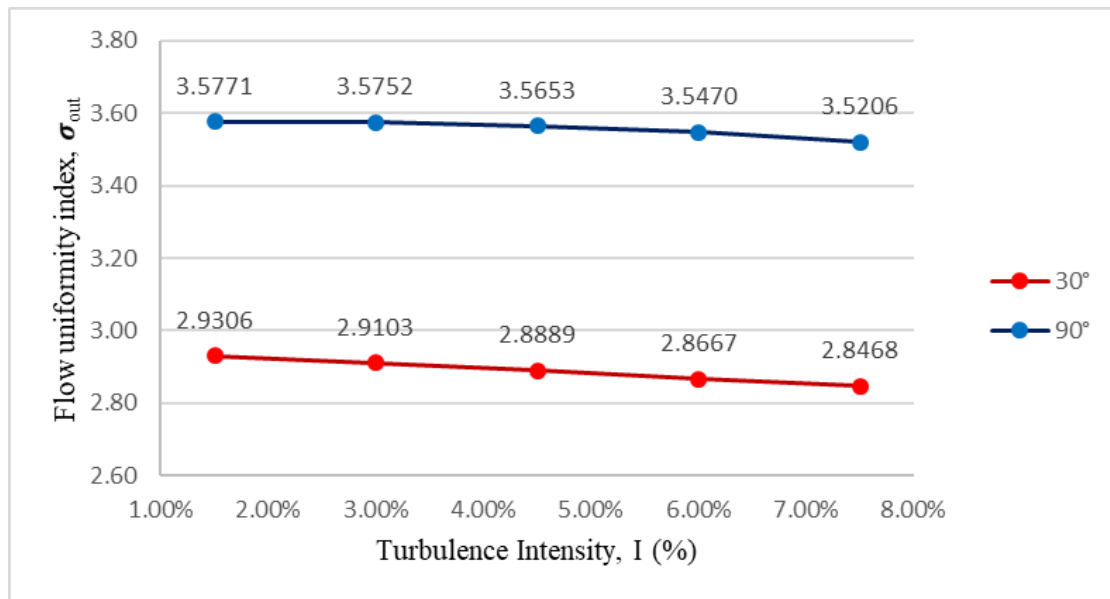


Fig. 12. Comparison of  $\sigma_{out}$  versus  $I$  at 30° and 90° turning diffusers

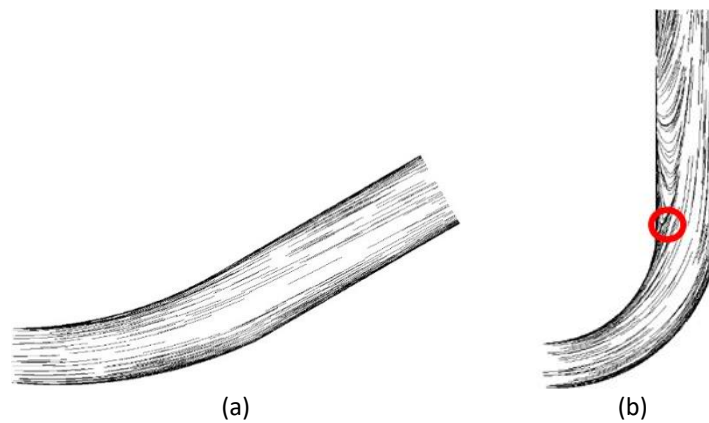


Fig. 13. Flow separation in (a) 30° and (b) 90° turning diffuser with turbulence intensity of 7.50%

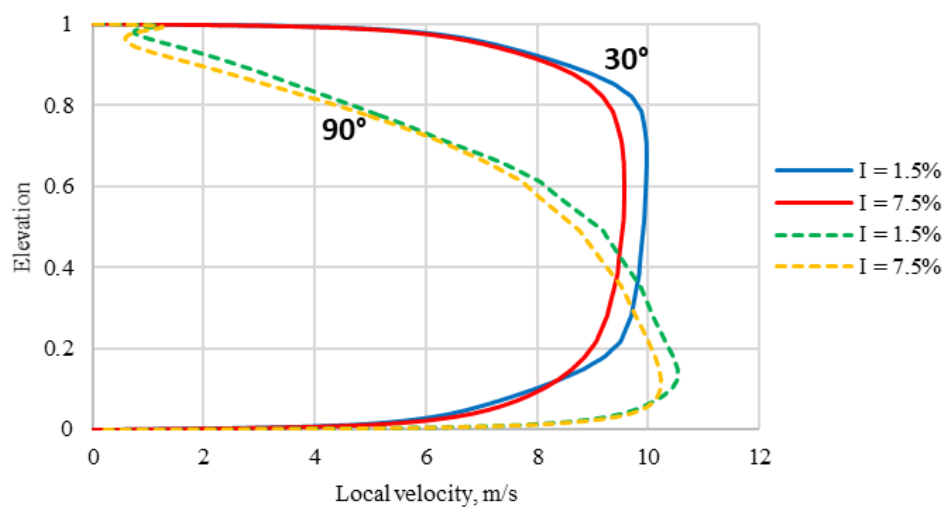


Fig. 14. Comparison of velocity profile versus outlet width for both 30° and 90° when applying min  $I=1.5\%$  and max  $I=7.5\%$

## 4. Conclusions

In conclusion, performances of 3-D turning diffuser can be affected by the operating parameter and geometrical but it can be improved by application of turbulence intensity. Based on this study, performances of both turning diffuser of flow uniformity and pressure recovery had shown an enhancement on the fluid flow of turning diffusers. A 7.5% of turbulence intensity are highly recommended to introduce in the ducting flow application so as to improve the flow performance of pressure recovery and uniformity of flow.

## Acknowledgement

This research was supported in part by Universiti Tun Hussein Onn Malaysia under Fundamental Research Grant Scheme (FRGS) Vote K102. The CFD work was conducted in CFD Laboratory, Universiti Tun Hussein Onn Malaysia (UTHM).

## References

- [1] Nordin, Normayati, Abdul Karim, Zainal Ambri, Safiah Othman, and Vijay R. Raghavan. "Effect of varying inflow Reynolds number on pressure recovery and flow uniformity of 3-D turning diffuser." In *Applied Mechanics and Materials*, vol. 699, pp. 422-428. Trans Tech Publications, 2015.
- [2] Li, Angui, Changqing Yang, Tong Ren, Xin Bao, Erwei Qin, and Ran Gao. "PIV experiment and evaluation of air flow performance of swirl diffuser mounted on the floor." *Energy and Buildings* 156 (2017): 58-69.
- [3] Sinha, Prasanta K., A. K. Biswas, A. N. Mullick, and B. Majumdar. "Flow development through a duct and a diffuser using CFD." *Int J Eng Res Appl* 7 (2017): 46-54.
- [4] Fox, Robert W., and S. J. Kline. "Flow regimes in curved subsonic diffusers." *Journal of Basic Engineering* 84, no. 3 (1962): 303-312.
- [5] Hoffmann, J. A., and G. Gonzalez. "Effects of small-scale, high intensity inlet turbulence on flow in a two-dimensional diffuser." *Journal of Fluids Engineering* 106, (1984): 121-124.
- [6] Sullerey, R. K., Brajesh Chandra, and V. Muralidhar. "Performance comparison of straight and curved diffusers." *Defence Science Journal* 33, no. 3 (1983): 195-203.
- [7] Mahalakshmi, N. V., G. Krithiga, S. Sandhya, J. Vikraman, and V. Ganesan. "Experimental investigations of flow through conical diffusers with and without wake type velocity distortions at inlet." *Experimental Thermal and Fluid Science* 32, no. 1 (2007): 133-157.
- [8] Khong, Y. T., N. Nordin, S. M. Seri, A. N. Mohammed, A. Sapit, I. Taib, K. Abdullah, A. Sadikin, and M. A. Razali. "Effect of turning angle on performance of 2-D turning diffuser via Asymptotic Computational Fluid Dynamics." In *IOP Conference Series: Materials Science and Engineering*, vol. 243, no. 1, p. 012013. IOP Publishing, 2017.
- [9] Jakirlić, S., G. Kadavelil, M. Kornhaas, M. Schäfer, D. C. Sternel, and C. Tropea. "Numerical and physical aspects in LES and hybrid LES/RANS of turbulent flow separation in a 3-D diffuser." *International Journal of Heat and Fluid Flow* 31, no. 5 (2010): 820-832.
- [10] Tham, Wei Xian, Normayati Nordin, Azian Hariri, Nurul Fitriah Nasir, Norasikin Mat Isa, Musli Nizam Yahya, and Suzairin Md Seri. "Asymptotic Computational Fluid Dynamic (ACFD) Study of Three-Dimensional Turning Diffuser Performance by Varying Angle of Turn." *International Journal of Integrated Engineering* 11, no. 5 (2019): 109-118.
- [11] Nordin, Normayati, Safiah Othman, Vijay R. Raghavan, and Zainal Ambri Abdul Karim. "Verification of 3-D stereoscopic PIV operation and procedures." *International Journal Engineering and Technology IJET/IJENS* 12, no. 4 (2012): 19-26.
- [12] Bourgeois, Jason A., Robert J. Martinuzzi, Eric Savory, Chao Zhang, and Douglas A. Roberts. "Assessment of turbulence model predictions for an aero-engine centrifugal compressor." *Journal of Turbomachinery* 133, no. 1 (2011): 011025.
- [13] Nguyen, Cuong K., Tuan D. Ngo, Priyan A. Mendis, and John CK Cheung. "A flow analysis for a turning rapid diffuser using CFD." In *4th International Symposium on Computational Wind Engineering*, (2006).
- [14] Nordin, Normayati, and BANDAR SERI ISKANDAR. "Performance investigation of turning diffusers at various geometrical and operating parameters." PhD diss., Universiti Teknologi Petronas, 2016.
- [15] Selamat, Ubaidullah, Kahar Osman, Arul Hisham A. Rahim, and Selamat Ubaidullah. "Heat and Flow Analysis of a Chilled Water Storage System using Computational Fluid Dynamics." *Journal of Advanced Research in Fluid Mechanics and Thermal Sciences* 57, no. 1 (2019): 131-140.

- 
- [16] Nordin, N., S. M. Seri, I. Taib, A. N. Mohammed, M. K. Abdullah, and A. Sapit. "Secondary flow vortices and flow separation of 2-D turning diffuser via particle image velocimetry." In *IOP Conference Series: Materials Science and Engineering*, vol. 226, no. 1, p. 012149. IOP Publishing, 2017.
- [17] Chong, T. P., P. F. Joseph, and P. O. A. L. Davies. "A parametric study of passive flow control for a short, high area ratio 90deg curved diffuser." *Journal of Fluids Engineering* 130, no. 11 (2008): 111104.
- [18] Abe, K., M. Nishida, A. Sakurai, Yuji Ohya, Hisashi Kihara, E. Wada, and K. Sato. "Experimental and numerical investigations of flow fields behind a small wind turbine with a flanged diffuser." *Journal of wind engineering and industrial aerodynamics* 93, no. 12 (2005): 951-970.